

General Disclaimer

One or more of the Following Statements may affect this Document

- This document has been reproduced from the best copy furnished by the organizational source. It is being released in the interest of making available as much information as possible.
- This document may contain data, which exceeds the sheet parameters. It was furnished in this condition by the organizational source and is the best copy available.
- This document may contain tone-on-tone or color graphs, charts and/or pictures, which have been reproduced in black and white.
- This document is paginated as submitted by the original source.
- Portions of this document are not fully legible due to the historical nature of some of the material. However, it is the best reproduction available from the original submission.

Rail Accelerator Technology and Applications

(NASA-TM-86947) RAIL ACCELERATOR TECHNOLOGY
AND APPLICATIONS (NASA) 18 p HC A02/MF A01
CSCL 21H

N85-21258

Unclas
14417

G3/20

Lynnette M. Zana and William R. Kerslake
Lewis Research Center
Cleveland, Ohio



Prepared for the
1985 JANNAF Propulsion Meeting
sponsored by the JANNAF Interagency Propulsion Committee
San Diego, California, April 9-12, 1985

NASA

RAIL ACCELERATOR TECHNOLOGY AND APPLICATIONS

Lynnette M. Zana and William R. Kerslake
National Aeronautics and Space Administration
Lewis Research Center
Cleveland, Ohio 44135

ABSTRACT

Rail accelerators offer a viable means of launching ton-size payloads from the Earth's surface to space. This paper presents the results of two mission studies which indicate that an Earth-to-Space Rail Launcher (ESRL) system is not only technically feasible but also economically beneficial, particularly when large amounts of bulk cargo are to be delivered to space.

An in-house experimental program at the Lewis Research Center (LeRC) has been conducted in parallel with the mission studies with the objective of examining technical feasibility issues. A 1 meter long - 12.5 x 12.5 mm bore rail accelerator was designed with clear polycarbonate sidewalls to visually observe the plasma armature acceleration. The general character of plasma/projectile dynamics is described for a typical test firing.

INTRODUCTION

The basic rail accelerator configuration is shown in Fig. 1. It consists of two long, parallel rails with a conducting armature (solid or plasma) between the two. Current flowing through one rail, across the armature, and returning through the other rail will generate a magnetic field. The interaction of the current with the field between the rails produces a Lorentz force ($J \times B$) which accelerates the armature. A projectile placed in front of the armature, then, can be accelerated with a force proportional to the current squared. Specifically,

$$F = \frac{1}{2} L' I^2 \quad (1)$$

where L' is the inductance per unit length of the accelerator and I is the current.

Electromagnetic launcher concepts date back to the early 1900's but received little notable attention until 1972 when researchers at the Australian National University used a 500 MJ homopolar generator to accelerate a 3 g mass to 5.9 km/sec in 3 m.^{1,2} The demonstration that gram-size projectiles could be accelerated to high velocities resulted in widespread interest for larger scale applications including ballistic weaponry, nuclear fusion, and space propulsion.

A rail accelerator research program at the Lewis Research Center (LeRC) has been completed. The objective of the program was to assess the use of rail accelerators for various in-space and to-space propulsion applications. The program focused on two main efforts: (1) mission defining studies to establish technical merit and estimate cost benefits, and (2) in-house research to examine technical feasibility issues.

An early mission study³ proposed a continuously firing, small bore rail accelerator as a means of low thrust orbit transfer. Gram-size pellets were accelerated to velocities of 5 to 20 km/sec to produce reactive thrust for spacecraft propulsion. Further concept evaluation was discontinued because only a marginal economic advantage existed over competitive ion propulsion systems (which already had an existing technology base) and because of projectile disposal problems.

A second mission study⁴ examined the use of rail accelerators in launching ton-size payloads directly from the Earth's surface to space. The study defined and assessed a conceptual Earth-to-Space Rail Launcher (ESRL) capable of fulfilling two candidate missions: (1) space disposal of nuclear waste, and (2) delivery of bulk cargo to low Earth orbit (LEO). The ESRL system required a 2 km long rail accelerator operating with distributed energy totalling 1 TJ (10^{12} J). The required payload velocities for the two missions are 20 km/sec and 5 to 10 km/sec, respectively.

A follow-on study⁵ focused on near-term mission applications requiring the delivery of bulk cargo, such as to a Space Station (necessary launch velocity of 6.9 km/sec). However, in addition to rail accelerators, it considered all types of electromagnetic launcher (EML) concepts, the most promising of which is the coaxial magnetic accelerator. The use of an EML-coaxial hybrid was also studied in which the EML served as the first stage (1 to 2 km/sec) and chemical rockets provided the second and third stages.

The first part of this paper presents the rail accelerator mission concepts of Refs. 4 and 5, along with a summary of the technology and economic benefit assessments. The second portion of this paper describes the rail accelerator research conducted in-house.

One objective of the in-house research program was to understand the physics of plasma armatures over a scaling range sufficient to anticipate the performance of the meter-size bore accelerators required by an Earth-to-Space Rail Launcher system. To this end, small (4 x 6 mm) and medium (12.5 x 12.5 mm) bore accelerators have been tested in-house.⁶ This paper describes a typical test firing using a 1 m long - 12.5 x 12.5 mm bore rail accelerator. It was designed with clear polycarbonate sidewalls to permit visual observation of the plasma armature acceleration. Streak camera photography was used to characterize arc formation and acceleration. Details of the test design, diagnostic techniques, and overall performance will also be discussed.

SYMBOL LIST

Action	time integral of current squared, A ² -sec
B	magnetic field, Tesla
ESRL	Earth-to-Space Rail Launcher
F	Lorentz force, N
HPG	homopolar generator
I	current, A
L'	inductance gradient, H/m
L _{eff}	effective inductance gradient, H/m
LEO	low Earth orbit
MT	metric ton
m	mass, kg
OTV	orbit transfer vehicle
v _f	final projectile velocity, m/sec

MISSION STUDIES

BATTELLE STUDY I

In 1982, Battelle Columbus Laboratory⁴ assessed the potential feasibility and benefits of a conceptual Earth-to-Space Rail Launcher (ESRL) system capable of a variety of mission applications. The primary application, that of deep-space disposal of nuclear waste, required a launch velocity of 20 km/sec at a maximum of 10 000 g's acceleration. The secondary application, earth-to-orbit launching of nonfragile cargo, required velocities of 5 to 10 km/sec at 2500 g's.

The ESRL system was envisioned to be a multipurpose facility located on a remote island near the equator. Figure 2 gives an overview of the facility and the mission payloads. The facility would consist of two separate rail accelerators, each 2 km long. The accelerator for the primary mission (MISSION A) would be a vertical launcher tube with a 0.67 m² bore; for the secondary mission (MISSION B), the launcher would have a 1.0 m² bore and would be inclined 20° from the horizontal. The 20° elevation angle is a tradeoff between atmospheric drag and minimum launch velocity.

The rail launcher operates with distributed energy, totalling ~1 TJ (10¹² J). This would be supplied from a dedicated nuclear power plant located near the ESRL site. The launchers themselves would consist of two parallel conductors (amzirc), divided into 10,200 rail segments. Each segment would have its own 60 MJ homopolar generator/inductor unit. The units would spiral along the length of the launcher as shown in the figure. With this multistage configuration, the necessary acceleration energy could be distributed along the entire length of the launcher and switched into each segment as the projectile/armature travels down the launcher. In this manner, bore stresses would be minimized and launcher efficiency increased.

The study focused on the time frame from 2020 to 2050. At that time, as much as 0.5 MT (2 launches/day) of high-level nuclear waste from U.S. commercial plants and defense uses could be launched into solar system escape. As shown in Fig. 2, the nuclear waste projectiles have a blunted tungsten nose cone, which is expected to partially ablate away during flight through the atmosphere. The projectile is 1.7 m long and has a 12 cm thick steel shield to limit radiation. A high strength, ceramic sabot supports the projectile while in the launcher tube and thermally insulates it from the plasma armature. The sabot drops off once the projectile exits the launcher. Fins are added to

provide in-flight stability. Once launched at 20 km/sec, no onboard propulsion is needed. The projectile is tracked via ground-based and satellite systems. In case of a misfire, a monitoring system triggers an aerobraking decelerator to allow a low velocity reentry into the atmosphere. The total mass of the projectile (with a 250 kg payload) is 2055 kg.

The projectile for Mission B applications is also shown in Fig. 2. It is similar in configuration to the nuclear waste projectile except that it is longer (3.6 m) and wider (1.0 m diameter) and can carry a 650 kg payload. The total mass is 6500 kg. The Mission B projectiles must have an onboard propulsion system for orbit circularization. Approximately 5.2 MT of bulk material (cargo/consumables/propellant) could be delivered to Earth orbit at a rate of eight launches per day.

Cost estimates for the above Earth-to-Space Rail Launcher system performing both Missions (A) and (B) range from 5 to 8 billion dollars (1981). This includes research, development, and investments with a 30 yr amortization. Annual operating expenses are expected to be 60 million dollars. At two launches per day, it would cost 560 dollars/kg to dispose of nuclear waste. At a rate of eight launches per day, the cost of launching bulk cargo to Earth orbit would be 590 dollars/kg.

The first Battelle study concluded that an Earth-to-Space Rail Launcher system was not only technically feasible but also environmentally and economically beneficial. At the time this study was completed, however, the U.S. decided to bury all nuclear waste in mined geological repositories so the prime mission application was no longer viable.

BATTELLE STUDY II

Battelle conducted a follow-on study⁵ investigating all types of electromagnetic launchers (EMLs) in addition to rail accelerators. The study emphasized near-term applications, focusing on the missions which required the delivery of bulk cargo to space, such as to a space station. The EML types included the coaxial magnetic accelerator, the electrothermal thruster (ramjet), an electromagnetic rocket gun, and an electromagnetic theta gun. An EML - chemical hybrid was also studied in which the EML served as the first stage (1 to 2 km/sec) and chemical rockets provided the second and third stages.

Of all electromagnetic launcher types studied, only the coaxial magnetic accelerator showed promise equal to or superior to that of a rail accelerator. The coaxial magnetic accelerator and its concept development are described in detail in Ref. 5; however, only rail accelerator concepts will be presented here.

Seven candidate missions were identified as having possible rail accelerator application. These are: Earth-orbital launch, lunar base supply, solar system escape, Earth escape, suborbital launch, SSTO/TAV boost, and space-based launch. The merit of a particular mission model was predicated on the need for a large amount of payload to be delivered. After preliminary evaluation of the seven missions, the Earth-orbit launch was selected for development as a reference concept because it had the largest material delivery requirements.

The Earth-orbit mission model supports an orbiting Space Station with delivery of supply items, Orbit Transfer Vehicle (OTV) propellants, and materials for space processing facilities. It assumes a significant manned presence aboard the station by the year 2020. Projected personnel growth is estimated at 16 people by the year 2000, 100 people by the year 2020, and increasing to 250 people by 2050. A higher model predicts 750 personnel in space in the year 2050.

EARTH TO ORBIT RAIL LAUNCHER

The Earth-to-Orbit Rail Launcher concept to support the above mission model is shown in Fig. 3. As in the first Battelle study, the launcher is 2 km long with a 1 m² bore. The launcher would be based on a mountain side at an elevation angle of 20° from the horizontal. A system of 3600 homopolar generator/inductor units, distributed evenly along the length of the launcher would supply the necessary acceleration energy. A dedicated nuclear power plant again supplies power to the system. Structural support of the launcher would be provided by a concrete foundation as shown in the figure.

The projectiles would weigh 5900 kg with a 650 kg payload. It would be launched at a velocity of 6.9 km/sec at a maximum of 1225 g's acceleration. An on-board propulsion system would provide the additional 2 km/sec necessary for orbit insertion at a 500 km altitude.

Total research, development, and investment costs for the Earth-to-Orbit Rail Launcher are estimated at 2.2 billion dollars (1981). Annual operations costs are expected to be 40 million dollars. The large capital expenditure reduces the cost effectiveness of the rail launcher for low launch rates. For example, at a launch rate of one 650 kg payload per day, the cost per kilogram would be 757 dollars when amortized over a 30 yr period. However, at a rate of 10 launches per day the cost would be 234 dollars/kg.

HYBRID RAIL ACCELERATOR/ROCKET

A hybrid rail accelerator/rocket could also support the Earth-orbital mission model. Figure 4 provides an overview of the system. The rail launcher would be situated at a 35° angle from the horizontal and would again be 2 km long with a 1 m diameter round bore. The round bore allows the projectile to be spin-stabilized. Energy to the launcher would be provided by 750 homopolar generator/inductor units (42 GJ total energy). At a maximum of 100 g's acceleration, the projectiles would be launched at a velocity of 2 km/sec. After a short coast period, the projectile second stage (rocket first stage) is ignited, then jettisoned after burn is completed. The third stage ignites and is jettisoned after burn-out while the fourth stage puts the payload into its proper orbit.

Figure 4 also shows the hybrid projectile. It is 12 m long with a 1 m diameter and can carry an 800 kg payload. The initial mass of the projectile would be 15,000 kg. Approximately 13,000 kg of solid propellant is required for the second and third stages and for orbit insertion.

Total investment cost for a hybrid rail accelerator/rocket system is expected to be 1.3 billion dollars (1981) with a 40 million dollar annual operations cost. A rate of one launch per day results in an amortized cost of 559 dollars/kg payload. At 10 launches per day, the cost drops to 216 dollars/kg.

Figure 5 compares hypothetical total program costs for the hybrid rail accelerator/rocket system to conventional launchers including a four-stage rocket (800 kg payload), the current STS, and an unmanned launch vehicle (ULV). At low launch rates, a four-stage rocket would be more economical than the hybrid system. Assuming a 1.5 billion dollar program cost, at least three launches a day are needed to justify development of a hybrid rail accelerator/rocket.

TECHNOLOGY ASSESSMENT

Both the first and second Battelle studies concluded that large-scale applications of rail accelerators were technically feasible. However, they did identify several areas requiring technology development. Of critical importance is the scale-up of existing rail accelerator systems. To date, rail accelerators that have been tested are only a few meters long with centimeter-size bores. (The Los Alamos HYVAX rail accelerator, designed for velocities of 15 km/sec, is 13 m long. Also, Westinghouse launched a 317 g mass to 4.2 km/sec.⁷) Another area of primary concern is the distribution and switching of mega-ampere currents into the launcher as the projectile accelerates in-bore. (The University of Texas at Austin Center for Electromechanics (UT-CEM), demonstrated a 4 m long, 10 stage rail accelerator. A 1 g mass was accelerated to 3 km/sec.⁸) Projectile design considerations are another critical technology issue. The high accelerations of launch (100 to 2500 g's) place added constraints on materials selection, structural integrity, and aerothermodynamics. Other technology development areas of importance include: (1) testing and development of sabot concepts; (2) further study of plasma and solid armatures; (3) investigation of projectile/bore and sabot/projectile friction during launch; and (4) more experimental work in the use of preboost systems to reduce rail erosion.

IN-HOUSE RAIL ACCELERATOR RESEARCH

APPARATUS AND PROCEDURE

The LeRC rail accelerator facility uses a 240 KJ system of capacitor banks matched to an inductive impedance to provide accelerating currents of up to 500 KA. Figure 6 gives an electrical schematic of the circuit. The capacitor bank system is charged by a single power supply and can provide varying capacitances from 1.27 to 5.06 mF at up to 10 kv. Upon discharge of the banks, large crowbar ignitions prevent ringing of the circuit, i.e., huge current and voltage reversals. Reference 9 describes the design, installation, and operating characteristics of the facility. Details of the 1 m long, small (4 x 6 mm) and medium (12.5 x 12.5 mm) bore rail accelerator designs tested in-house and diagnostic techniques used are given in Ref. 10. Reference 6 contains the results of 145 test firings conducted in 1984.

Figure 7 displays a cross section of the 12.5 x 12.5 mm bore accelerator. The bore is defined by two half-hard copper rails (12.5 x 18.5 mm) and two Lexguard® sidewalls. Lexguard® is a high strength, clear polycarbonate with a laminated, mar-resistant surface. A fiberglass epoxy (G-10) is used as the outer insulation piece. Phenolic compression plates clamp the entire structure; the clamping action is against the outward rail forces under impulsive loading. The geometric L' of this rail configuration is $0.52 \mu\text{H/m}^{11}$ (dc) and is $0.38 \mu\text{H/m}$ in the high frequency limit.¹² Due to skin effects, the actual value tends toward the high frequency limit. For a typical test current pulse, an average, instantaneous value was determined to be $0.43 \mu\text{H/m}$.¹³

The projectile is a clear lexan cube, 12.4 x 12.4 x 13.5 mm long, and is hand-fit to bore dimensions (Fig. 8). It has a 9.09 mm diameter hole drilled in at the front of the projectile to a point 3.2 mm from the rear. This reduces projectile mass and moves the center of mass to the rear of the cube to help prevent chattering while in-bore. A 1.6 mm thick piece of black rubber serves

as a seal (obturator) at the back face to help prevent plasma blowby. The projectile's starting position is 10 cm downstream of the accelerator breech. A piece of aluminum foil serves as a short across the rails during charge of the capacitor banks (2 A current). Upon firing it vaporizes and generates the plasma armature. The projectile, with obturator and foil, weighs 1.81 g. A G-10 cube plugs the breech of the accelerator to take advantage of gas dynamic forces to help projectile acceleration.

During a test firing a variety of diagnostic techniques are used to record the electrical characteristics of the accelerator and system as well as to obtain information on arc/projectile dynamics in-bore. A Pearson Model No. 2093 current transformer and a Rogowski coil are used to measure system and rail currents, respectively. Resistive divider networks are used to record the breech and arc voltage of the accelerator.

Information on arc/projectile performance in-bore is obtained by three different techniques. A set of dB/dt probes stationed at regular intervals along the length of the accelerator is used to establish the arc's position as a function of time. Each probe is a magnetic flux coil consisting of five wire turns wound on a nonmagnetic rod. The axis of the probe is positioned parallel with the accelerator bore so that it detects only the field associated with the plasma arc. The probe produces a voltage proportional to the time rate of change of the magnetic field (dB/dt). As the arc (and projectile) approach the probe station the flux in the coil increases. The direction of the flux through the coil reverses once the arc has passed the station. The zero crossings on the probe voltage output, then, indicate that the arc centroid is in line with the station.^{10,14}

A second in-bore diagnostic technique consists of a set of fiber optic probes embedded in the Lexguard® inner structure with epoxy and coupled to a photo transistor. The light pipes, located every 20 cm along the length of the accelerator, respond to the luminous plasma wavefront.

A high speed streak camera is also used to photograph plasma acceleration through a port in the test chamber as seen in Fig. 9. The streak camera is located in the picture foreground. Figure 10 details camera operation. The streak camera looks at an uninterrupted section of the accelerator from the breech to a position 80 cm downstream. The filmstrip rotates on a 27 cm diameter drum at a rate of ~130 -ps. (The film strip moves perpendicular to the arc motion by means of relay lenses and a relay mirror, however, the filmstrip moves perpendicular to the arc motion.) Time resolution to 4×10^{-7} sec can be obtained at writing speeds up to 0.13 mm/usec. As the arc travels down the bore, it paints a streak across the film. The dark lines on the film strip mark accelerator bolt locations so arc wavefront position versus time data may be obtained. The slope of the streak gives wavefront velocity.

A velocity stage (time of flight device) located one meter downstream of the muzzle gives final projectile velocity. The projectile is caught in a stack of ceiling tiles backed by an aluminum plate.

Overall accelerator performance can be quantified by use of an effective inductance gradient, L_{eff} . Integrating Eq. (1) with respect to time and rearranging, we have

$$L_{eff} = \frac{2 m v_f}{Action} \quad (2)$$

where

v_f = final projectile velocity, and

$Action = \int_0^t i^2(t) dt$ and reflects energy input into the accelerator.

RESULTS AND DISCUSSION

One typical test firing, conducted at a moderate energy level (44 kJ), is described. Total circuit capacitance and inductance were 2.54 mF and 1.4 μ H, respectively. The bank fired at 5.86 kv.

The resulting current waveform is shown in Fig. 11 with a peak current of 225 kA at 90 μ sec. Total Action for this test firing was $9.65 \times 10^6 A^2 \text{ sec}$.

Figure 12 displays the arc/projectile position versus time plot as determined by the various diagnostics. The dB/dt probe data points, marking the arc centroid location, fall slightly behind the fiber optic data which respond to the arc wavefront, as expected. The fiber optic data, then, is a better indicator of projectile position while in-bore. It fits in well with the velocity stage timing marks.

The arc half-length increases from 1 cm at the initial stages of acceleration to ~7.5 cm halfway downstream. This agrees with theoretical predictions of arc length.¹⁵

Streak camera data, corrected for parallax, is also plotted in the figure. The shaded area corresponds to the most intense region of arc luminosity. The leading edge of this region carries the largest portion of current density as evidenced by corresponding dB/dt data points. At a position 47 cm downstream of the breech there is a distinct split between projectile motion and the arc centroid path (as indicated by an arrow in the photo). The projectile stops accelerating at 60 cm and coasts out the muzzle. This would be expected as the current is only one-tenth of its peak value at this point. However, the arc has actually decoupled from the projectile and is decelerating.

This arc deceleration phenomenon can be more readily seen in the streak photo of Fig. 13(a). One possible explanation is an arc-ablative process in which rail-sidewall material is eroded by the high temperature (10^4 °K) arc¹⁵ and then ionized. This mass addition to the arc/projectile system inhibits accelerator performance.¹⁶

The streak photo also shows a faint, luminous wavefront moving in front of the projectile. This luminosity is caused by the compression of air ahead of the projectile. The air is partially warmed by hot plasma leaking past the projectile. Little actual current, though, is associated with this particular wavefront as the dB/dt coils did not sense any noticeable flux change.

However, at higher current loadings, (or after several test firings when the G-10 structure pieces have fatigued) the outward rail forces create larger gaps between the projectile and the bore sidewalls. More plasma blows by, creating a conductive, secondary current path. Up to half of the rail current may be diverted (or shorted) through this forward plasma. This heavy blowby case is also more luminous as shown in Fig. 13(b).

For this test firing, the projectile exited the accelerator at 1010 μ sec with a final velocity of 1150 m/sec. Using Eq. (2) gives an L_{eff} of 0.43 μ H/m. This equals the average, instantaneous value calculated earlier.

Typical performance parameters for the 12.5 x 12.5 mm bore accelerator design, however, generally range from 0.30 to 0.49 μ H/m. The large spread in L_{eff} values and the fact that the lowest parameter falls well under the inductance gradient for the high frequency limiting case (0.38 μ H/m) is believed to be caused by several factors: (1) the arc ablative phenomenon mentioned above; (2) progressive crack formation and delamination of the G-10 outer structure leading to gas pressure leakage; and (3) compression of the barrel material leading to excessive bore clearance with plasma blowby.

SUMMARY

NASA space propulsion mission studies have shown that rail accelerators are technically feasible and economically/environmentally beneficial as an Earth-to-Space Rail Launcher. The most viable mission application is the delivery of bulk cargo (such as nonfragile supplies, OTV propellants, and materials for space processing) to an orbiting Space Station. The need for such an ESRL system, however, is predicated on a large material delivery requirement; economic payoff is not anticipated until the post 2020 era.

A typical firing of a 1 m long, 12.5 x 12.5 mm bore accelerator was described. A 1.8 g projectile was accelerated to 1150 m/sec in 0.9 m. Diagnostic techniques, including streak camera photography, were also presented.

The LeRC rail accelerator research program has been terminated due to the lack of near-term economical mission applications. Technical documentation of 145 rail accelerator firings conducted in-house is presented in Ref. 6.

REFERENCES

1. Rashleigh, S.C.; and Marshall, R.A.: Electromagnetic Acceleration of Macroparticles to High Velocities. J. Appl. Phys., vol. 49, no. 4, Apr. 1978, pp. 2540-2542.
2. Barber, J.P.: The Acceleration of Macroparticles and a Hypervelocity Electromagnetic Accelerator. Australian National University, Department of Engineering Physics, EP-T12, 1972.
3. Bauer, David P.; Barber, John P.; and Vahlberg, C. Julian: The Electric Rail Gun for Space Propulsion. NASA CR-165312, 1981.
4. Rice, E.E.; Miller, L.A.; and Earhart, R. W.: Preliminary Feasibility Assessment for Earth-to-Space Electromagnetic (Rail gun) Launchers. NASA CR-167886, 1982.
5. Miller, L.A.: Preliminary Analysis of Space Mission Applications for Electromagnetic Launchers. NASA CR-174748, 1984.

6. Zana, L.M.; Kerslake, W.R.; and Sturman, J.L.: Rail Accelerator Tests at Lewis Research Center. (to be published as a NASA document)
7. Deis, D.W.; Scherbarth, D.W.; and Ferrentino, G.L.: EMACK Electromagnetic Launcher Commissioning. IEEE Trans. Mag., vol. 20, no. 2, Mar. 1984, pp. 245-248.
8. Holland, L.D.: Distributed-Current-Feed and Distributed-Energy-Store Railguns. IEEE Trans. Mag. vol. 20, no. 2, Mar. 1984, pp. 272-275.
9. Gooder, Suzanne T.: Electromagnetic Propulsion Test Facility. NASA TM-83568, 1984.
10. Zana, L.M., et al.: LeKC Rail Accelerators: Test Designs and Diagnostic Techniques. IEEE Trans. Mag., vol. 20, no. 2, Mar. 1984, pp. 324-327.
11. Grover, F.W.: Inductance Calculations. D. Van Nostrand, New York, 1946.
12. Kerrisk, J.F.: Current Distribution and Inductance Calculations for Rail-Gun Conductors, LA-9092-MS, Los Alamos National Laboratory, 1981.
13. Author's calculations, unpublished.
14. Jamison, K.A.; and Burden, Henry S.: Arc Armature Diagnostic Experiments on an Electromagnetic Gun. Arradcom Technical Conference, July 1982.
15. Powell, John D.; and Batteh, Jad H.: Plasma Dynamics of an Arc-Driven, Electromagnetic, Projectile Accelerator. J. Appl. Phys., vol. 52, no. 4, Apr. 1981, pp. 2717-2750 (Author's calculations)
16. Parker, J.V.; and Parsons, W.M.: Effect of Ablation on Plasma Armature Dynamics. Presented at DARPA/Service Electromagnetic Propulsion Program Review, (Arlington, VA) Sept. 18-20, 1984.

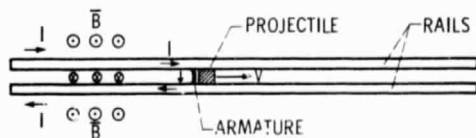


Figure 1. - Basic rail accelerator configuration.

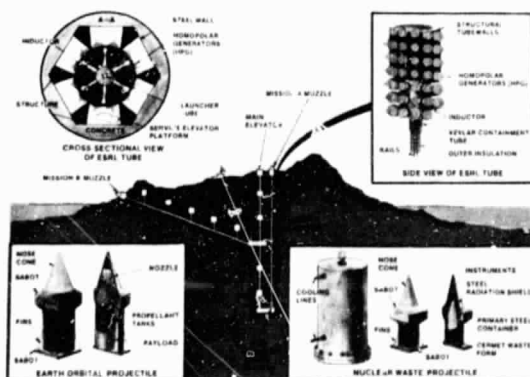


Figure 2. - Overview of ESRL launcher system and projectiles.

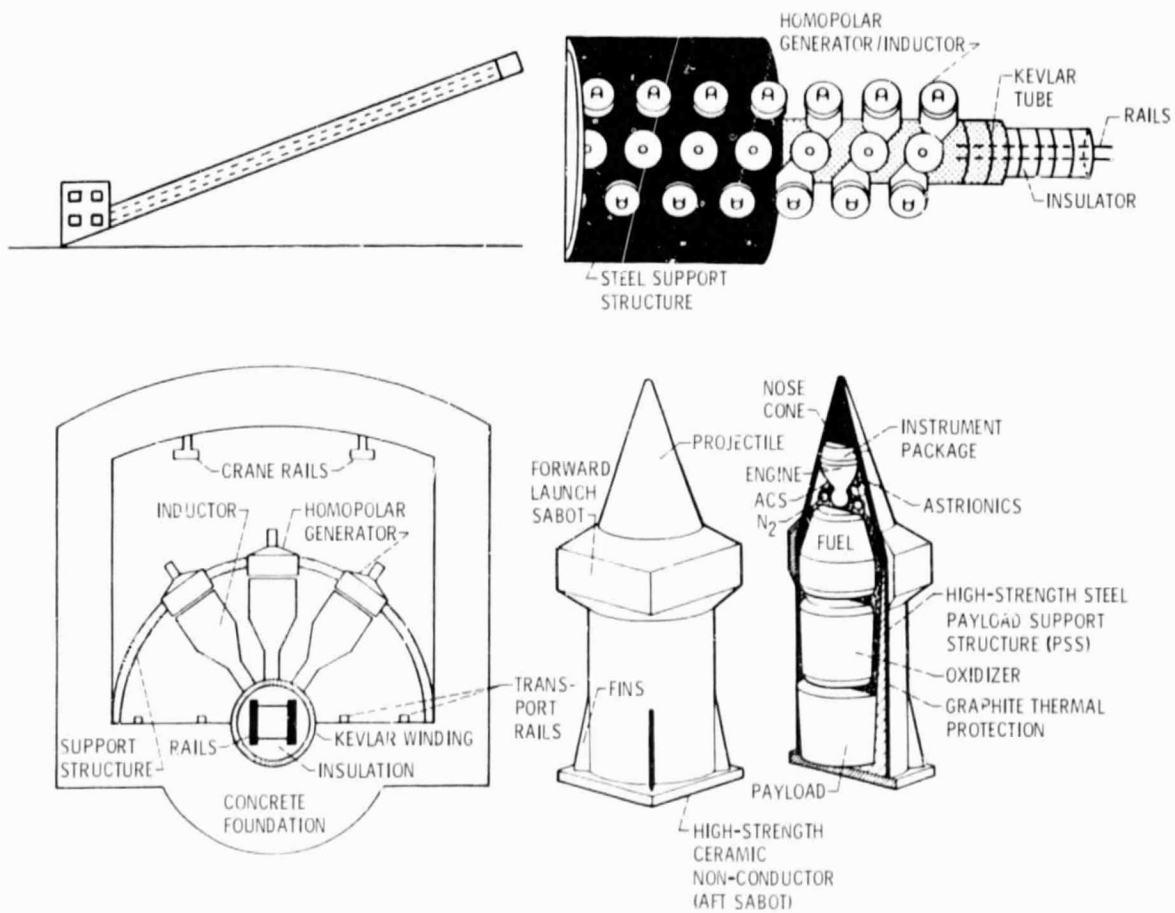


Figure 3. - Overview of the earth-to-orbit rail launcher concept.

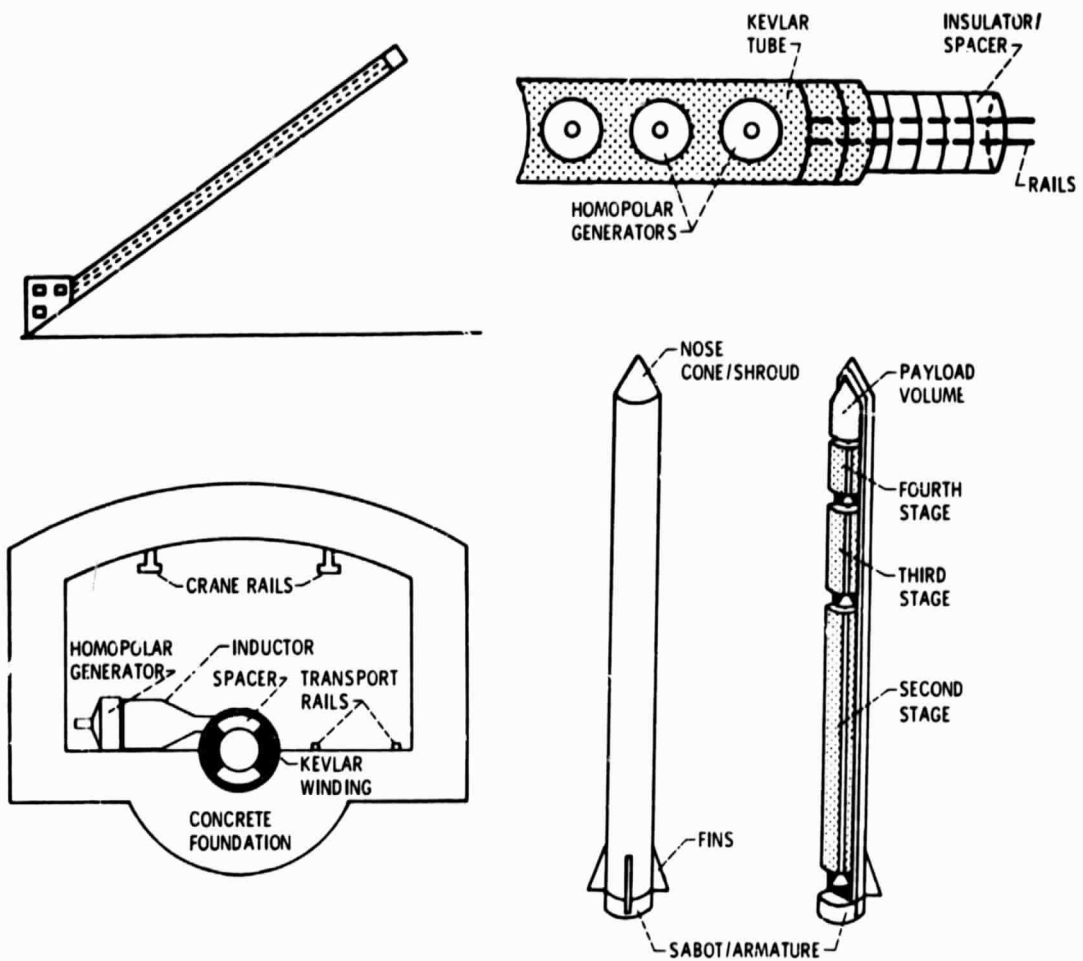


Figure 4. - Overview of the hybrid railgun/rocket concept.

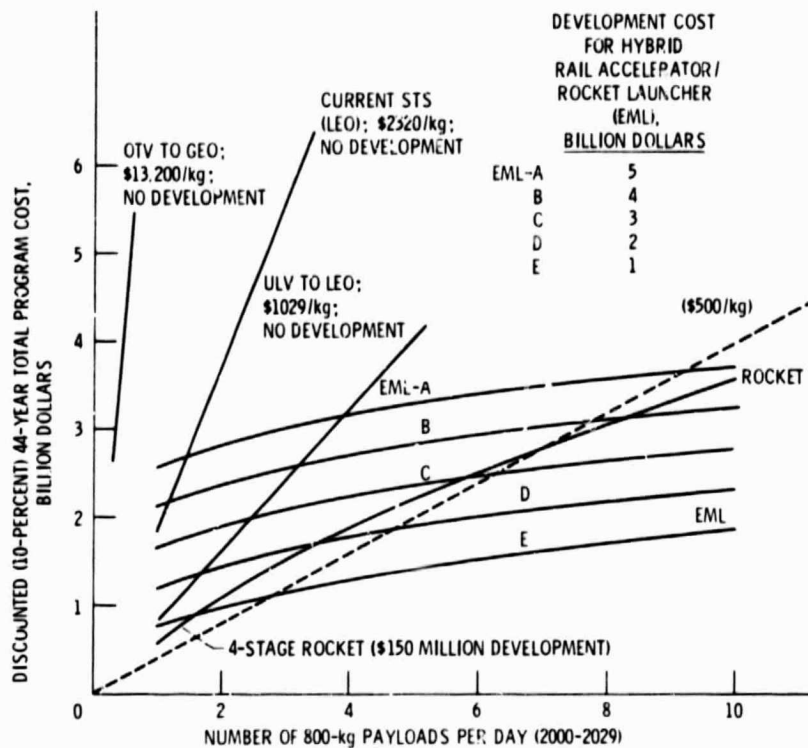


Figure 5. - Comparison of total program costs. Development years 1-14, 1986-1999; operation years 15-44, 2000-2029.

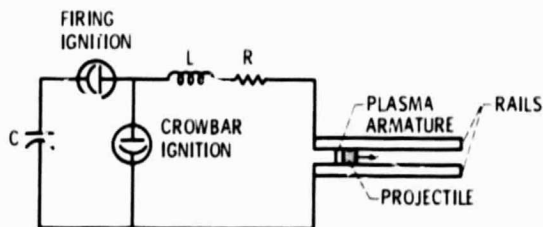


Figure 6. - Electrical schematic for pulsed power energy system.

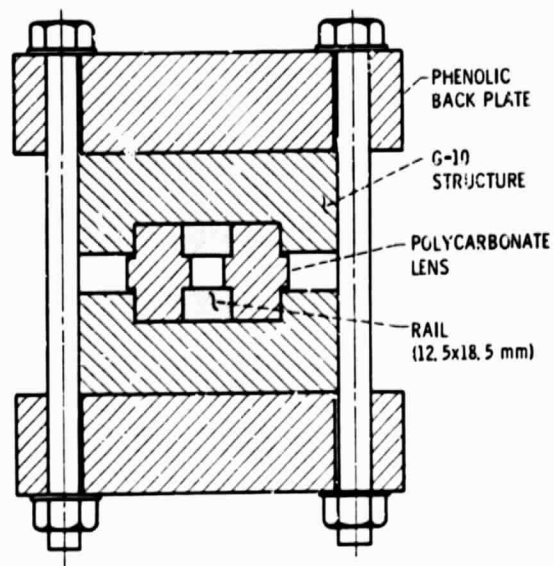


Figure 7. - 1 meter long, 12.5x12.5 mm bore rail accelerator.

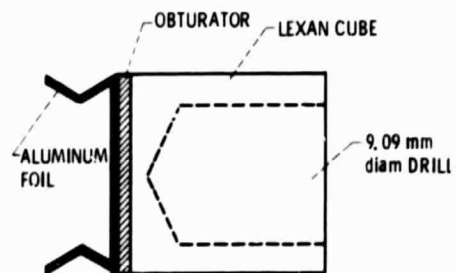


Figure 8. - Side view of projectile.

ORIGINAL PAGE IS
OF POOR QUALITY.

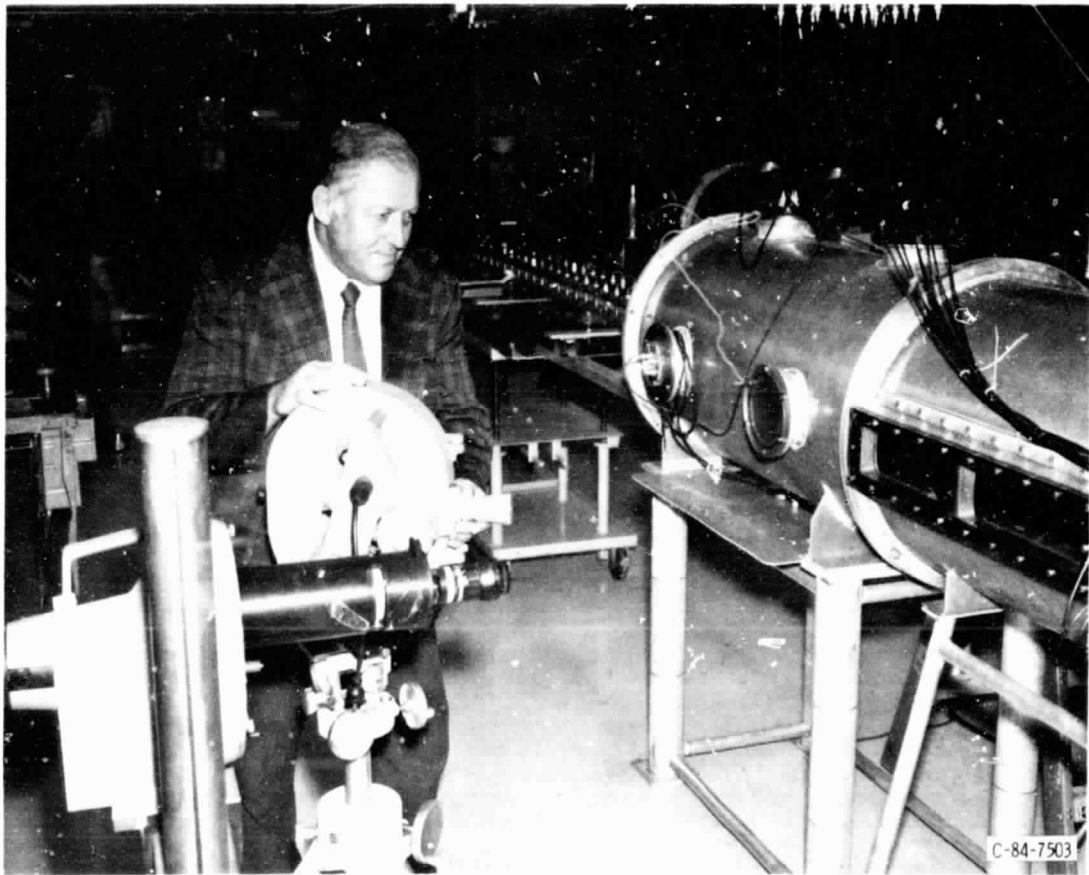
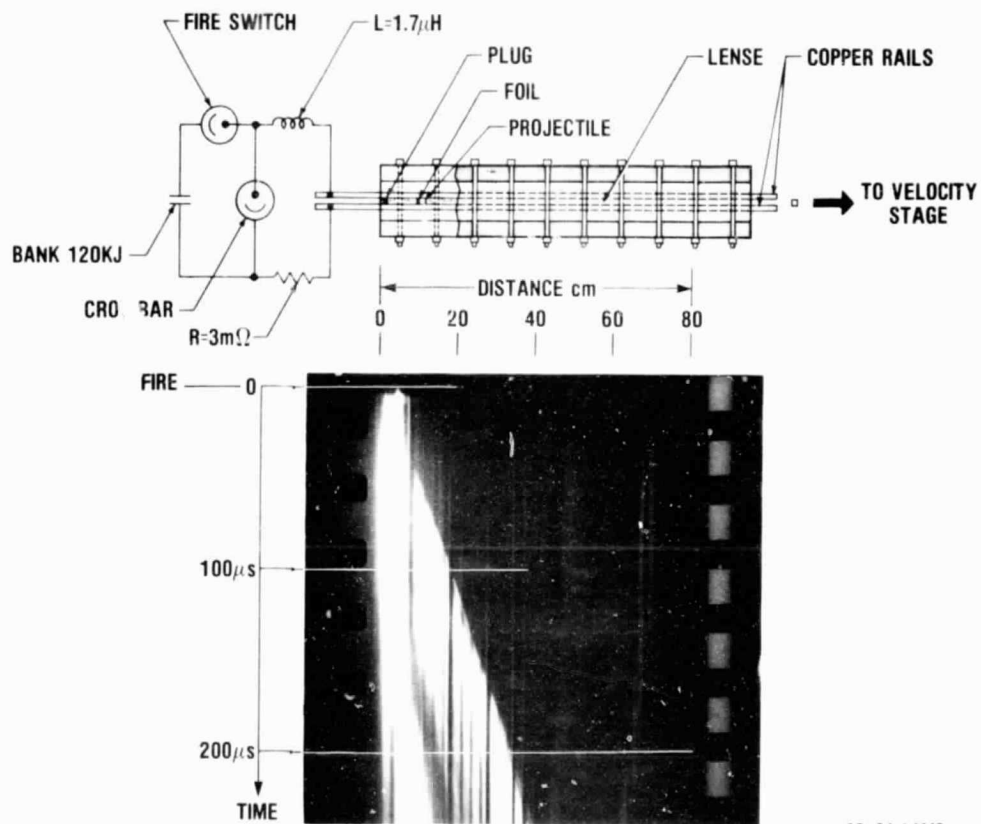


Figure 9. - Streak camera set-up.

ORIGINAL PAGE IS
OF POOR QUALITY



CD-84-14660

Figure 10. - Streak photography of 1-meter long accelerator.

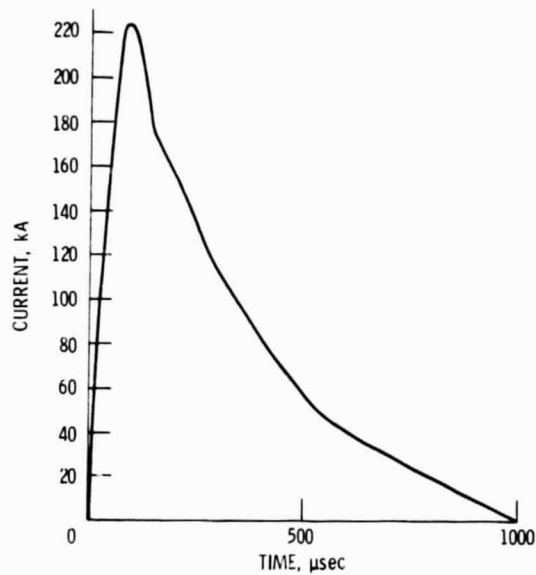


Figure 11. - Current versus time profile.

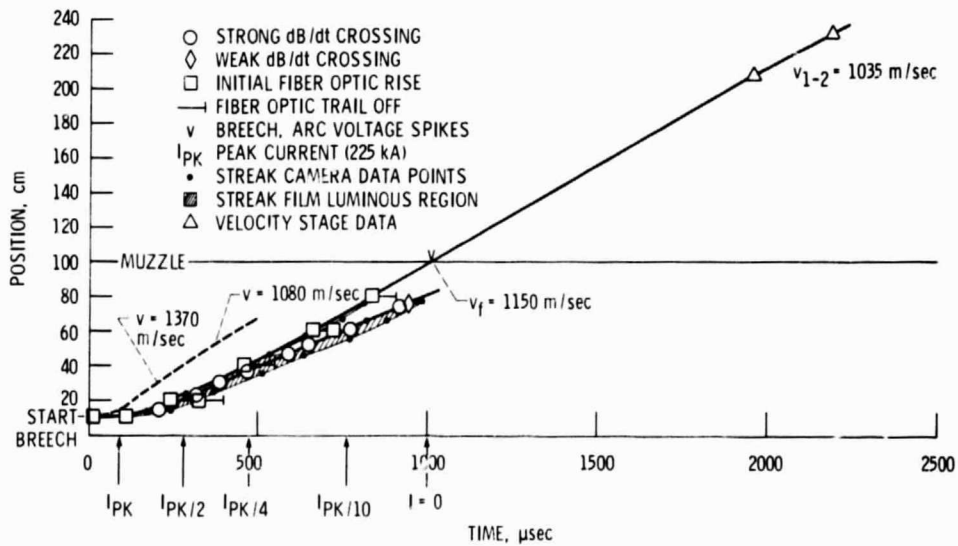


Figure 12. - Test number 105, position versus time.

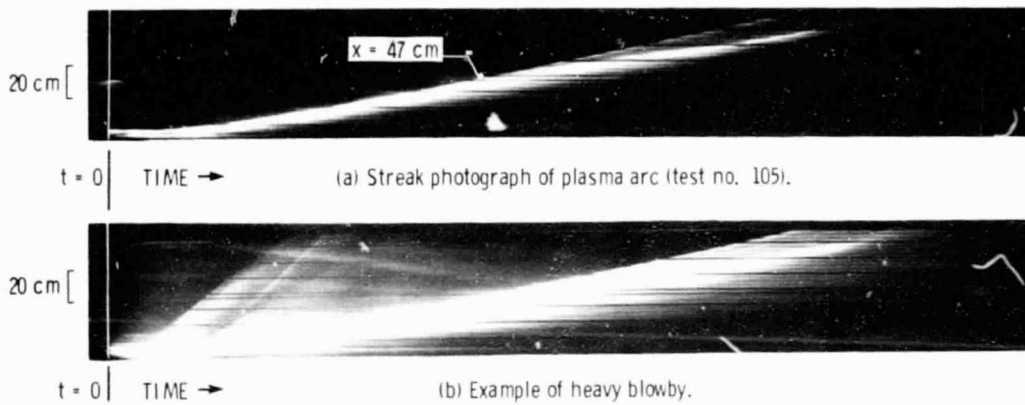


Figure 13. - Streak camera photography of plasma acceleration.